2025 International Symposium on Nonlinear Theory and Its Applications,
NOLTA2025, Naha city, Okinawa, Japan, October 27-31, 2025

Investigation of Relationship Between Spectral Radius and Echo State Property in Reservoir Computing

Hyuga Katsura†, Yoko Uwate†, and Yoshifumi Nishio†

†Department of Electrical Engineering, Tokushima University
2-1, Minamijosannjima, Tokushima-shi, Tokushima 770-8506, Japan
Email: c612434053@tokushima-u.ac.jp, uwate@ee.tokushima-u.ac.jp, nishio@ee.tokushima-u.ac.jp

Abstract—This study investigates the phenomenon that the Echo State Property (ESP) holds in regions with spectral radius $\rho > 1$, despite theoretical requirements to the contrary in reservoir computing. Through experiments using the Mackey-Glass equation, we confirmed that the saturation property of the tanh function suppresses the divergence of internal states, enabling ESP to hold in the range $1.0 < \rho < 1.7$. In this range, good performance was achieved with prediction accuracy (NRMSE) of about 0.12.

1. Introduction

Reservoir Computing (RC) is a type of recurrent neural network that shows high performance in time series prediction and dynamic system learning[1]. Among RC methods, Echo State Networks (ESN) are characterized by high computational efficiency, with fixed reservoir connection weights and training only the output layer weights. The Echo State Property (ESP), a crucial condition for ESN, refers to the property where internal states converge to the same values when given the same input from different initial states. This property enables ESN to appropriately retain past input information while making stable predictions.

Theoretically, the spectral radius ρ (maximum absolute eigenvalue) of the connection weight matrix must be less than 1. However, previous studies report that ESP holds even with $\rho > 1$ in chaotic time series prediction, achieving the highest accuracy[2, 3]. This contradiction between theory and experimental results may be explained by the saturation property of the tanh function used in the reservoir[3]. The tanh function output asymptotically approaches ± 1 as input magnitude increases. Due to this saturation property, internal state divergence may be suppressed even when $\rho > 1$, potentially allowing ESP to hold.

The objective of this study is to clarify the range where ESP holds for $\rho > 1$ and identify the spectral radius range where the saturation property functions. This bridges the gap between theory and experimental results, providing clearer ESN design guidelines.

ORCID iDs Hyuga Katsura: 0009-0009-4847-1278, Yoko Uwate: 0000-0002-2992-8852, Yoshifumi Nishio: 0000-0002-0247-0001

2. Proposed Method

2.1. Experimental Setup

The structure of the ESN is shown in Fig. 1. ESN consists of three layers: input layer, reservoir, and output layer, where nodes in the reservoir form a sparsely connected network. The number of nodes in the reservoir is set to 100, the connection probability to 0.2, and the leak rate to 0.3.

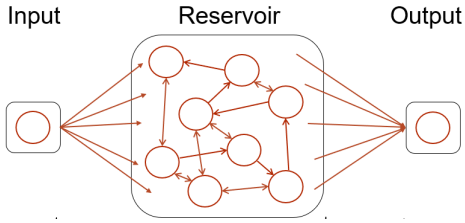

Figure 1: The structure of ESN.

The state update equation for the reservoir is as follows:

$$\mathbf{x}(t+1) = (1-\alpha)\mathbf{x}(t) + \alpha \cdot \tanh(\mathbf{W}\mathbf{x}(t) + \mathbf{W}_{\text{in}}\mathbf{u}(t+1)) \quad (1)$$

where x(t) represents the internal state of the reservoir, W is the node connection weight matrix, u(t) is the input time series, and $\mathbf{W}_{in}$ is the input weight matrix. The tanh function serves as the activation function, generating the nonlinear dynamics of the reservoir.

The Macky-Glass equation for chaotic time series to be used as input is as follows.

$$\frac{dx}{dt} = \beta \frac{x(t-\tau)}{1 + x(t-\tau)^{\gamma}} - \alpha x(t) \quad (2)$$

The parameters are set as $\beta = 0.2$, $\tau = 17$, $\gamma = 10$, and $\alpha = 0.1$, and 800 time series data points are generated. Of these, 600 are used as training data and 200 as test data.

2.2. Experimental Procedure

The experiment consists of the following three steps:

Step 1.

The spectral radius (ρ) is gradually increased from 0.9 to 4.0, and the prediction accuracy for the Mackey-Glass equation at each ρ is evaluated. The normalized root mean square error (NRMSE) is used as an indicator of prediction accuracy.

Step 2.

At each time step, the number of nodes for which $|tanh(Wx(t) + W_inu(t + 1))| > 0.90$ is counted, and the average value is calculated as the average saturation rate. As shown in Fig. 2, the tanh function enters the saturation region where the output exceeds 0.9 when the absolute value of the input exceeds approximately 1.47. Using this threshold, we quantify the proportion of nodes in the reservoir that are in the saturation region of the tanh function.

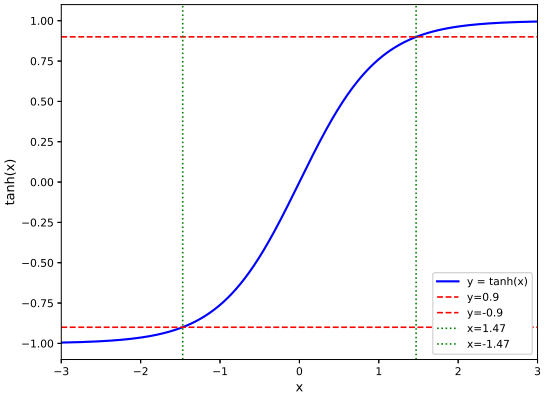

Figure 2: Saturation region of the tanh function.

Step 3.

Using two different initial states (randomly generated within the interval [-0.5, 0.5]), we observe how the difference in internal states changes. Specifically, for each of the N nodes, we calculate the difference in values between the two initial states and evaluate the establishment of ESP by their average value. A simple calculation example of the initial state difference is shown in Fig. 3.

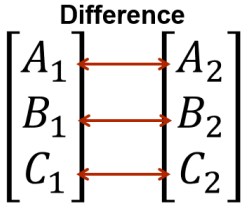

Figure 3: Calculation of initial state difference.

In addition, to account for the influence of the pseudo-random number generator's initial value, experiments are conducted using 10 different initial values, and the average is taken as the final result.

3. Simulation Results

3.1. Prediction Accuracy and Spectral Radius

The transition in prediction accuracy as ρ is gradually increased is shown in Fig. 4. The horizontal axis is ρ and the vertical axis is NRMSE, which indicates the prediction accuracy. The results of 10 different initial values are plotted individually, with the average shown as a green line.

In the range $0.9 < \rho < 1.0$, high prediction accuracy (NRMSE < 0.13) is obtained for all initial values. This indicates that ESP holds for $\rho < 1$ as theoretically expected, enabling stable prediction.

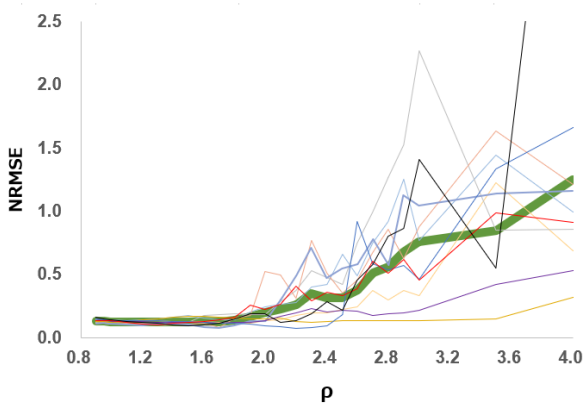

Figure 4: Prediction accuracy for each ρ.

Notably, in the range $1.0 < \rho < 1.8$, similarly high prediction accuracy is maintained for all initial values. In particular, the highest prediction accuracy (NRMSE = 0.12327) is recorded around $\rho = 1.2$. This suggests that even in the region $\rho > 1$ where ESP theoretically should not hold, the divergence of internal states is suppressed by the saturation property, enabling stable prediction.

On the other hand, in the range $1.8 < \rho < 4.0$, large variations in prediction accuracy are observed depending on the initial values, and the average prediction accuracy also decreased rapidly. This is thought to be because the amplification of internal state differences exceeded the suppression effect of the saturation property, causing ESP to no longer hold.

3.2. Analysis of Average Saturation Rate

The transition in average saturation rate when ρ is gradually increased is shown in Fig. 5. The horizontal axis is ρ and the vertical axis is average saturation rate. The results of 10 different initial values are plotted individually, with the average shown as a green line.

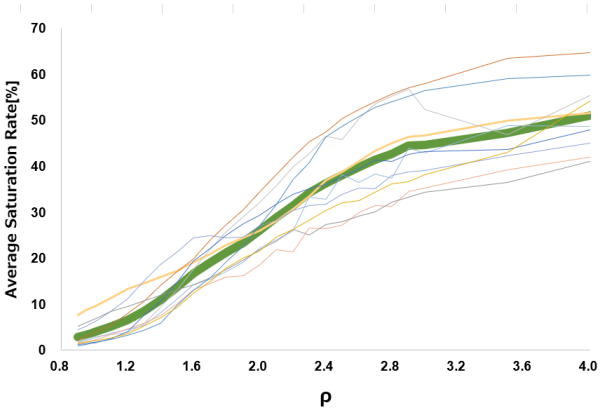

Figure 5: Average saturation rate for each ρ.

In the range $0.9 < \rho < 1.0$, the average saturation rate showed low values of less than 5%. This means that the output values of most nodes are in the linear region of the tanh function.

In the range $1.0 < \rho < 1.8$, the average saturation rate increased from about 5% to 20%. In this range, it is thought that an appropriate number of nodes entering the saturation region effectively suppresses the divergence of internal states. The results suggest that when the average saturation rate is up to about 20%, the saturation property functions appropriately and contributes to the establishment of ESP.

On the other hand, in the range $1.8 < \rho < 4.0$, large variations in prediction accuracy were observed depending on the initial values, and the average prediction accuracy also decreased rapidly. This is thought to be because the amplification of internal state differences exceeded the suppression effect of the saturation property, causing ESP to no longer hold.

3.3. Verification of Echo State Property

A heat map of the differences in internal states when using two different initial states is shown in Fig. 6. The horizontal axis represents the spectral radius, and the vertical axis represents the time step. The darker the blue, the smaller the internal state difference, and the darker the red, the larger the internal state difference.

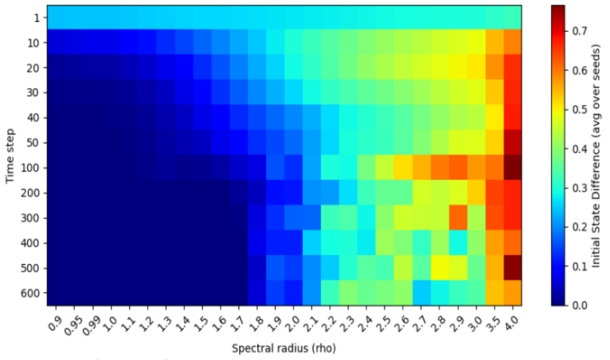

Figure 6: The heatmap of internal state difference.

On the left side of the heat map (the area where $0.9 < \rho < 1.0$), it can be observed that the color rapidly changes to blue in the first few steps, and the internal state difference quickly converges to 0. This indicates that the system has strong contractility, as predicted by conventional theory. On the other hand, when $\rho > 1$, the convergence speed gradually slows down, but eventually reaches blue at around $\rho = 1.7$.

The most interesting thing is that, in the range of $1.0 < \rho < 1.2$, the decay pattern of the initial state difference changes from a smooth exponential decay to a more complex non-linear decay. This suggests that the system is transitioning from a linear region to a non-linear region, and that saturation properties are gradually beginning to have an effect.

At the final 600 time steps, it is confirmed that the internal state difference converges to 0 (shown in dark blue) in the range of $0.9 < \rho < 1.7$. In particular, in the range of $1.0 < \rho < 1.7$, it is clearly shown that the internal state difference converges to 0, even though ESP should not theoretically be valid.

A heat map focusing on the first 10 time steps, during which internal state differences changed dramatically, is shown in Fig. 7.

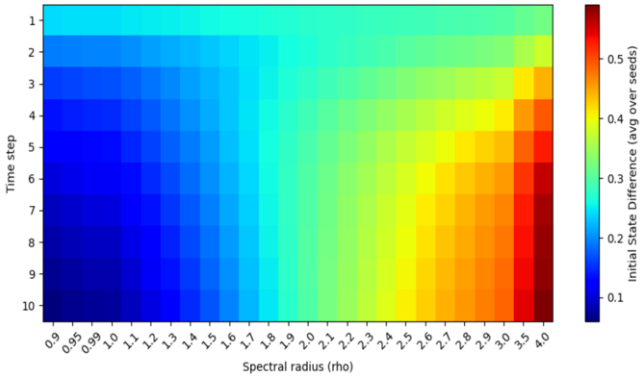

Figure 7: The heatmap focusing on the first 10 time steps.

At $\rho = 0.9$, the difference in internal states reaches nearly 0 in about 3 steps, whereas at $\rho = 1.5$, it takes about 8 steps to achieve the same degree of decay. This difference in decay rate reflects the strength of the system's contractility.

Additionally, in the region where $\rho > 1.2$,, subtle oscillations appear in the decay curve. This indicates that the interaction between nonlinear dynamics and saturation effects results in a complex transient response that deviates from simple exponential decay.

However, in the range where $\rho < 1.7$, these oscillations are temporary, and it is confirmed that the internal state difference ultimately converges to 0.

3.4. Identification of the Functional Range of Saturation Property

From the above results, it becomes clear that the range where the saturation property functions and ESP holds is $1.0 < \rho < 1.7$. In this range:

- Prediction accuracy (NRMSE): 0.12327–0.12619
- Average saturation rate: 3.92%–19.05%

4. Mechanisms of Saturation Property and Theoretical Considerations

4.1. Analysis of tanh Function Saturation Property

The core of the phenomenon observed in this study lies in the nonlinear characteristics of the tanh function. The tanh function enters a saturation region where the output exceeds 0.9 when the absolute value of input x exceeds

approximately 1.47. This property enables the following mechanisms:

Relationship between Linear and Saturation Regions: When $\rho < 1$, the majority of nodes (over 95%) operate in the linear region, and the system exhibits quasi-linear behavior. In contrast, for $1.0 < \rho < 1.7$, 5-20% of nodes enter the saturation region, introducing moderate nonlinearity.

Amplification Suppression Mechanism: For $\rho > 1$, internal state differences should theoretically amplify exponentially. However, due to the saturation property of the tanh function, the output growth rate decreases significantly relative to the input growth rate. Specifically, in the region $|x| > 3$, the derivative of $\tanh(x)$ becomes less than 0.01, substantially suppressing the effective amplification rate.

4.2. Identification of Critical Saturation Rate

The experimental results revealed that system behavior undergoes qualitative changes at a boundary of approximately 20% average saturation rate. This critical value is determined by the following factors:

Information Retention Capability: With saturation rates below 20%, over 80% of nodes can capture input changes linearly, appropriately representing fine variations in the time series.

Stability Assurance: Simultaneously, saturation of approximately 20% of nodes effectively suppresses system-wide divergence.

4.3. Theoretical Basis for Optimal Spectral Radius

The highest prediction accuracy (NRMSE = 0.12327) obtained near $\rho = 1.2$ results from the balance of two factors:

Memory Capacity Enhancement: When ρ exceeds 1, the effective memory capacity of the reservoir increases, enabling capture of longer-term temporal dependencies.

Stability Maintenance: Moderate saturation with an average saturation rate of 6.59% maintains rich dynamics while avoiding chaotic divergence.

These results represent phenomena unique to nonlinear systems that cannot be explained by conventional linear stability theory, providing new guidelines for reservoir computing design.

5. Conclusion

In this study, we investigated in detail the relationship between spectral radius and echo state property in reservoir computing, particularly the influence of saturation property in the region $\rho > 1$. While traditional theory requires $\rho < 1$ as a necessary condition for ESP, practical systems have been reported to achieve good performance beyond this constraint. This study provides important insights that bridge this gap between theory and practice.

The following important findings were obtained from the experiments:

1. Even in the region $\rho > 1$ where ESP theoretically should not hold, it was confirmed that ESP holds in the range $1.0 < \rho < 1.7$ due to the saturation property. This discovery suggests the need for extending the conventional theoretical framework.
2. In this range, by maintaining the average saturation rate below about 20%, the divergence of internal states is effectively suppressed, and high prediction accuracy is maintained. Notably, the optimal performance obtained around $\rho = 1.2$ is important as a practical design guideline.
3. For $\rho > 1.7$, excessive saturation prevents proper capture of input changes, ESP does not hold, and prediction accuracy decreases. This indicates that the saturation property has limits to its effective functioning.

These results indicate that in ESN design, rather than simply following the theoretical constraint of $\rho < 1$, more flexible design considering the saturation property is possible. Particularly for prediction of complex dynamic systems such as chaotic time series, the range $1.0 < \rho < 1.7$ with moderate saturation may be optimal.

Future research should investigate the influence of saturation properties on different activation functions such as ReLU and sigmoid functions. Mathematical modeling of the relationship between average saturation rate and prediction accuracy could establish more systematic guidelines for ESN design. Additionally, the effects of quantization for hardware implementation warrant further investigation.

Acknowledgments

This work was partly supported by JSPS KAKENHI Grant Number JP25K15273.

References

[1] Jaeger, H., Haas, H. (2004). Harnessing nonlinearity: Predicting chaotic systems and saving energy in wireless communication. Science, 304(5667), 78-80.

[2] Yildiz, I. B., Jaeger, H., Kiebel, S. J. (2012). Revisiting the echo state property. Neural Networks, 35, 1-9.

[3] Manjunath, G., Jaeger, H. (2013). Echo state property linked to an input: Exploring a fundamental characteristic of recurrent neural networks. Neural Computation, 25(3), 671-696.